



A new Fenton-like system for catalytic oxidation of crystal violet using Zn^0/Fe_3O_4

Huifang Tian^{a,b}, Guangming Zhang^{b,*}, Yifei Sun^a, Jia Zhu^c, Shan Chong^b, He Zhao^b, Ting Huang^b

^aSchool of Space and Environment, Beihang University, 37 Xueyuan Road, Beijing, China, Tel. 18813195418; email: thf90527@163.com (H. Tian), Tel. 82338120; email: sunif@buaa.edu.cn (Y. Sun)

^bSchool of Environment and Natural Resources, Renmin University of China, 59 Zhongguancun Avenue, Beijing, China, Tel. 86 10 82502680; email: zgm@ruc.edu.cn (G. Zhang), Tel. 18813053521; email: 396185870@qq.com (S. Chong), Tel. 15110186482; email: zhaoh628@163.com (H. Zhao), Tel. 18810463649; email: jason_huangting@163.com (T. Huang)

^cSchool of Construction and Environment Engineering, Shenzhen Polytechnic, Shenzhen, China, Tel. 86 755 26731000; email: 7566874@qq.com

Received 3 November 2017; Accepted 16 March 2018

ABSTRACT

A Zn^0/Fe_3O_4 composite catalyst was synthesized by co-precipitation and tested as a Fenton-like system for crystal violet decolorization. The prepared Zn^0/Fe_3O_4 catalyst was characterized by scanning electron microscopy, X-ray diffraction and vibrating sample magnetometry. The results indicated that Zn^0 was successfully distributed on Fe_3O_4 and that the composite showed a large specific surface area and high magnetic separation ability, the results also showed that the Zn^0/Fe_3O_4 crystallites size was about 32–45 nm. The Zn^0/Fe_3O_4 catalyst also showed high activity at neutral pH value. The effects of Zn^0/Fe_3O_4 dosage, hydrogen peroxide (H_2O_2) concentration and reaction time were optimized for the catalytic oxidation of crystal violet. The reaction of crystal violet in these Fenton-like systems followed a pseudo-first order reaction, with rate constants (k_{obs}) of 0.26, 0.19 and 0.02 min^{-1} for the $Zn^0/Fe_3O_4-H_2O_2$, Zn^0/H_2O_2 and Fe_3O_4/H_2O_2 systems, respectively. At neutral pH, the optimal conditions were identified as 0.7 g/L of Zn^0/Fe_3O_4 and 0.41 mmol/L of H_2O_2 . Under these conditions, 94% of crystal violet could be removed within 7 min. The lack of residual sludge is an advantage of this method. A decrease in the decolorization efficiency is observed when other synthetic dyes or common natural organic matters are present. Crystal violet was completely decolorized and mostly degraded by $Zn^0/Fe_3O_4-H_2O_2$ as measured with UV-Vis, HPLC and TOC. The $Zn^0/Fe_3O_4-H_2O_2$ system was shown to be a promising and highly efficient catalyst for the decolorization of crystal violet in water.

Keywords: Zn^0/Fe_3O_4 ; Hydrogen peroxide; Catalytic oxidation; Crystal violet; Decolorization efficiency

1. Introduction

In recent years, several advanced oxidation processes have been proposed for the treatment of organic pollutants in water. The Fenton reagent, comprising Fe^{2+} as a catalyst and hydrogen peroxide (H_2O_2) as an oxidant, is particularly promising for this application [1]. In an acidic medium,

hydroxyl radicals ($HO\cdot$) are produced from H_2O_2 , and these radicals rapidly oxidize organic contaminants [2]. However, the Fenton process produces a large volume of sludge, requiring further treatment and disposal [3]. Moreover, acidic conditions are harmful to aquatic organisms [4,5]. To overcome these disadvantages, supported iron catalysts, such as zero valent iron (Fe^0) [6,7], iron oxides ($\alpha-Fe_2O_3$, $\gamma-Fe_2O_3$, $\alpha-FeOOH$, $\gamma-FeOOH$) [8,9], Fe_3O_4 [10,11] and Fe^0/Fe_3O_4 [12], have been developed and tested.

* Corresponding author.

Despite their simplicity, the application of iron-based Fenton-like systems has been restricted by acidity and iron precipitation. To solve these problems, ongoing efforts have been devoted to exploring alternative non-iron Fenton catalysts. Recently, zinc-based catalysts, such as dysprosium-doped ZnO [13] and Gd-doped ZnO [14] in photocatalytic technology and ZnO-TiO₂ [15], ZnO [16] and Sm-doped zinc oxide [17] in sono-catalytic technology, have often been proposed for the removal of organic pollutants. Some other studies have reported that supported zinc metal catalysts showed high catalytic activity in Fenton-like systems in a wide range of pH [18,19].

Another issue is the separation and recycling of catalysts after the completion of the reaction due to its complexity, cost and production of sludge [20,21]. Some alternative strategies have been explored to solve this problem as well. It was reported that a magnetic material is one of the best options for the separation of the catalyst [22,23]. Additionally, Wang et al. [24] also reported that magnetic iron oxides demonstrated superior catalytic activity as well as high magnetic separation ability.

As a representative triphenylmethane dye, crystal violet is widely used in the dyeing industry and coloring oil, which has caused the presence of this substance in water environment [25–28]. Also, crystal violet is highly mutagenic and carcinogenic and is a mitotic poison for mammalian cells [29–31]. In this study, crystal violet was chosen as a model pollutant.

The aim of this work was to prepare a new catalyst, namely, zero valent zinc/magnetic iron oxide (Zn⁰/Fe₃O₄). The combination of zinc metal materials and iron oxides may provide the advantages of both high catalytic activity and good separation from water. In this study, we investigated the oxidation of crystal violet using Zn⁰/Fe₃O₄ and H₂O₂. The effects of important parameters, such as Zn⁰/Fe₃O₄ dosage, H₂O₂ concentration, pH range and reaction time, were investigated. Additionally, the interference of other synthetic dyes and common natural organic matter was also investigated. The objective of this study was to develop a new and effective Fenton-like method for the treatment of wastewaters and establish the optimum conditions for this method.

2. Materials and methods

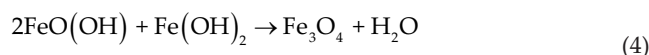
2.1. Materials

All chemicals used in this study were of analytical grade and were used without further purification. Crystal violet, methylene blue, methyl orange, fuchsin acid, L-malic acid, L-histidine and humic acid were obtained from Sinopharm Chemical Reagent Co., Ltd., China. Ferric chloride hexahydrate (FeCl₃·6H₂O), ferrous sulfate heptahydrate (FeSO₄·7H₂O), zinc sulfate heptahydrate (ZnSO₄·7H₂O), sodium borohydride (NaBH₄) and sodium hydroxide (NaOH) were purchased from Xilong Chemical Co., Ltd. H₂O₂ (30%, v/v) and ammonia solution (NH₃·H₂O, 28%, v/v) were obtained from Beijing Chemical Works. Nitrogen (N₂) gas was supplied by Beijing Aolin Gas Company.

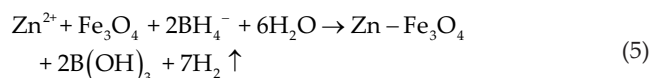
2.2. Preparation of the catalyst

Magnetite particles were synthesized by co-precipitation [32]. FeCl₃·6H₂O (8.9 mmol) and FeSO₄·7H₂O

(4.8 mmol) were dissolved in 20 mL deionized water under nitrogen for 10 min, and the resulting solution was added dropwise to 180 mL deionized water with NH₃·H₂O (0.04 mol) with a dropping rate of 3 mL/min, then stirring for 30 min under vigorous mechanical stirring. The following reactions occurred:



The freshly formed Fe₃O₄ was subsequently washed three times with ultrapure water to remove the residual iron ions and separated by a magnet. Fe₃O₄ was placed into a three-necked bottle with 100 mL deionized water, and then, 0.0269 mol ZnSO₄·7H₂O was added. Then, 200 mL 0.269 mol/L NaBH₄ aqueous solution was administered dropwise under mechanical stirring for 30 min. Thus, the Zn⁰/Fe₃O₄ composite was formed as described by Eq. (5).



2.3. Characterization of the catalyst

The surface morphology of the catalyst was investigated using an S-4700 scanning electron microscope (SEM) (Hitachi Ltd., Japan). X-ray diffraction (XRD) patterns of the catalyst were scanned over a 2θ range from 10° to 80° using a Bruker D8 Advance X-ray diffractometer (Bruker Corporation, Germany). Magnetic measurements were performed using a vibrating sample magnetometer (Quantum Design Inc., USA).

2.4. Experimental procedure

The catalytic activity of the Zn⁰/Fe₃O₄ composite was tested for decolorizing crystal violet. The analysis of crystal violet was performed using a UV-Vis absorption spectrophotometer (Purkinje General Corporation, TU-1900, China), and the absorption wavelength was set at 590 nm. The concentration of hydrogen peroxide (H₂O₂) was measured by iodometry. The initial concentration of crystal violet was 15 mg/L. The effect of the catalyst dosage was investigated in the range from 0 to 1.0 g/L. The effect of the H₂O₂ concentration was investigated in the range from 0 to 0.68 mmol/L. The effect of the reaction time was studied from 0 to 10 min. For the experiments in the presence of co-existing dyes, the total dye concentration was 15 mg/L. For the co-existing natural organic matter experiments, the total concentration was also set to 15 mg/L. For HPLC measurement, the conditions of HPLC were as follows: leachate: 9.0 mmol/L Na₂CO₃, flow rate: 1.0 mL/min, injection volume: 20 mL, wavelength: 584 nm, flow phase: V(CH₃OH):V(H₂O) = 7:3.

3. Results and discussion

3.1. Characterization of the Zn⁰/Fe₃O₄ catalyst

Scanning electron microscopy micrographs of Fe₃O₄ and Zn⁰/Fe₃O₄ are presented in Figs. 1(a) and (b), respectively, and it can be seen that the Fe₃O₄ particle showed dispersed irregularity structure, single particle showed columnar structure, whereas when zinc was loaded onto the Fe₃O₄ particle, the catalyst had a lamellar shape. This proves the incorporation of Zn⁰ over the surface of the Fe₃O₄ magnetite structure and verifies that the specific surface area was large, increasing the probability of contact with the dye molecules.

Fig. 1(c) shows the XRD patterns of the Fe₃O₄ and Zn⁰/Fe₃O₄ catalysts. The peaks at 25.68°, 35.17° and 60.71° were indexed as diffractions of (100) of Fe₃O₄ and those at 35.36° as diffractions of (101) of zero-valent zinc. These results indicated that zero-valent zinc was successfully loaded onto Fe₃O₄. It also seems that the change of peaks intensity in XRD pattern of Zn⁰/Fe₃O₄ was related to the location of Zn⁰. According to the following Scherrer equation (Eq. (6)) [33,34], the average size (*D*) of crystallites of the samples was estimated in the range of 32–45 nm.

$$D = k\lambda/\beta\cos\theta \quad (6)$$

In this equation, β is the peak half-width, k is the constant ($k = 0.89$), λ is the wavelength ($\lambda = 0.154056$) and θ is the incident angle of the X-rays.

A prominent advantage of the prepared Zn⁰/Fe₃O₄ catalyst is that it could be easily separated from water by an external magnet. The magnetic hysteresis loop is illustrated in Fig. 2. The saturation magnetization of Zn⁰/Fe₃O₄ is 16.65 emu/g and shows evidence of super-paramagnetism. Fig. 2 (inset)

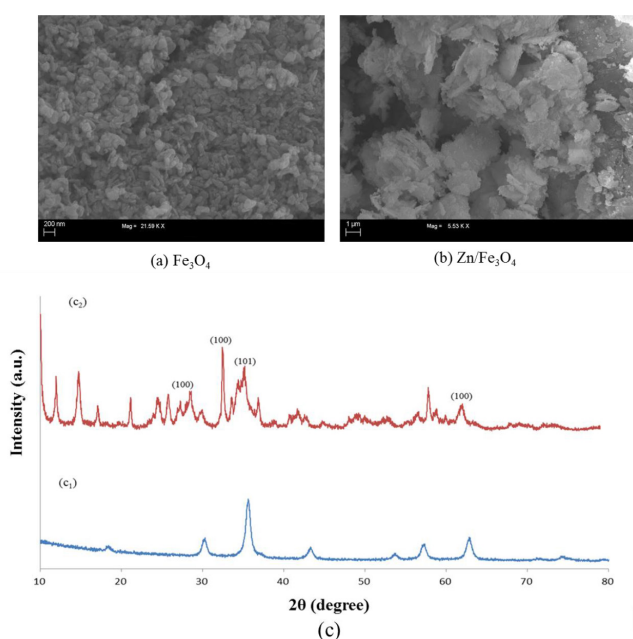


Fig. 1. Characterization of Zn⁰/Fe₃O₄ as a catalyst. (a) SEM image of the Fe₃O₄; (b) SEM image of the Zn⁰/Fe₃O₄ composite; (c) XRD profile of the Zn⁰/Fe₃O₄ composite with comparison with Fe₃O₄; (c₁) Fe₃O₄; (c₂) Zn⁰/Fe₃O₄.

verifies that the catalyst could be easily separated by using an external magnet, which is highly advantageous for the further application of this catalyst.

3.2. Catalytic activity of the Zn⁰/Fe₃O₄ catalyst

Experiments were conducted to demonstrate the catalytic activity for the decolorization of crystal violet. We first examined the efficiency of (i) zero-valent zinc, (ii) Fe₃O₄ and (iii) Zn⁰/Fe₃O₄ without H₂O₂. Fe₃O₄ shows little effect in the removal of crystal violet, while zero-valent zinc produced good reduction (Fig. 3(a)). The results indicated that adsorption was very low but that reduction played an important role. However, compared with zero-valent zinc, the reducibility of the Zn⁰/Fe₃O₄ composite diminished, indicating that Fe₃O₄ restrains the reducibility of zero-valent zinc.

H₂O₂ alone showed very poor performance (<5%) in crystal violet removal (Fig. 3(b)). A combination of Zn⁰/H₂O₂ showed a much better result, and the removal efficiency was higher than the sum of the efficiencies of zero-valent zinc and of H₂O₂ used separately. The results indicated that zero-valent zinc acts as a catalyst in this system, with Zn⁰ as a reductant and H₂O₂ as an oxidant. The Zn⁰/Fe₃O₄ composite had the highest catalytic activity, and the catalytic activity of zero-valent zinc was clearly promoted by Fe₃O₄. This finding is also very interesting because the reducibility of zero-valent zinc was decreased by Fe₃O₄ (Fig. 3(a)).

As shown in Fig. 3(c), Fe₃O₄ showed some catalytic activity in Fenton-like systems, indicating that it may contribute to crystal violet removal, in addition to providing easy separation after the reaction. Fig. 3(d) was the plot of $\ln(C/C_0)$ with reaction time in Zn⁰/Fe₃O₄-H₂O₂, Zn⁰/H₂O₂ and Fe₃O₄/H₂O₂ systems (d₁: linear segment of the curves used for calculation of k values). The reaction of crystal violet in these Fenton-like systems could be expressed by the Langmuir Hinshelwood kinetics curve [35,36], as shown in Fig. 3(d₁) and (d₂), the Zn⁰/Fe₃O₄-H₂O₂, Zn⁰/H₂O₂ and Fe₃O₄/H₂O₂ systems followed a pseudo-first order reaction, respectively, with rate constants (k_{obs}) of 0.26 ($R^2 = 0.9948$), 0.19 ($R^2 = 0.9958$) and 0.02

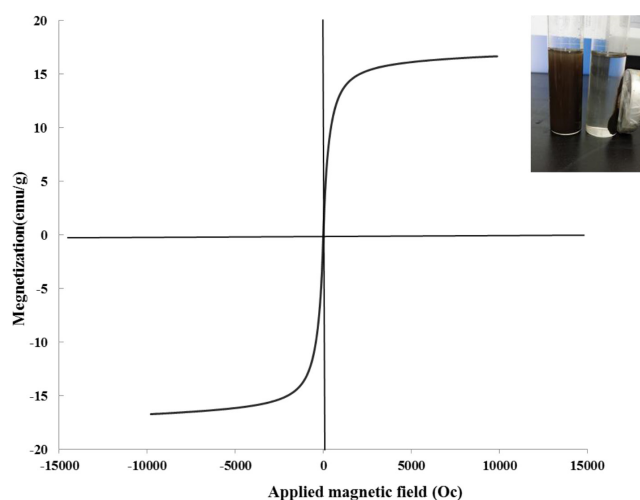


Fig. 2. Magnetization hysteresis loop of the Zn⁰/Fe₃O₄ composite (the photograph in the inset shows magnetic separation with an external magnet).

($R^2 = 0.9667$) min^{-1} . The catalytic activity of the $\text{Zn}^0/\text{Fe}_3\text{O}_4$ composite was higher than the sum of the activities of Fe_3O_4 and zero-valent zinc used separately, clearly showing a synergistic effect. This agreed with Costa et al.'s [12] finding in degradation of methylene blue in a $\text{Fe}^0/\text{Fe}_3\text{O}_4\text{-H}_2\text{O}_2$ system.

As a result, after 10 min, more than 95% of crystal violet was catalytically oxidized by $\text{Zn}^0/\text{Fe}_3\text{O}_4\text{-H}_2\text{O}_2$. Furthermore, no remaining H_2O_2 was detected after the reaction, indicating the high catalytic ability of $\text{Zn}^0/\text{Fe}_3\text{O}_4$ for the reduction of H_2O_2 . The lack of residual sludge production is another

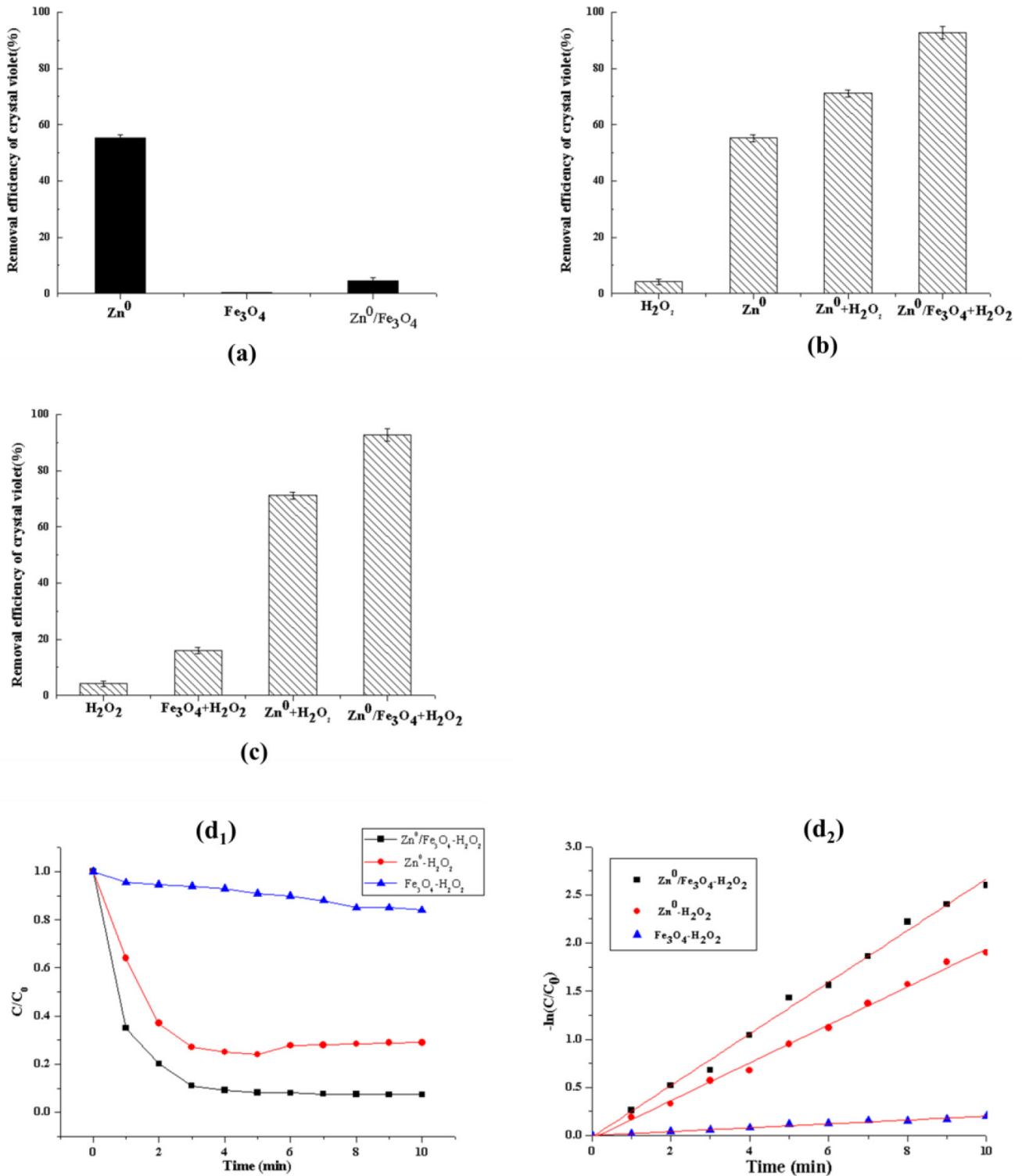


Fig. 3. Removal efficiency of crystal violet in different systems (15 mg/L crystal violet concentration, 1.0 g/L catalyst dosage, 0.68 mmol/L H_2O_2 , $t = 10$ min, $\text{pH} = 5.0$).

important advantage of this system, thus saving the trouble and costs of sludge treatment.

The reusability of the catalyst was also tested. As shown in Fig. 4, after the second time use of the catalyst, the removal efficiency of crystal violet was 7.56% lower than that of the first time, and the zinc concentration in water was 3.32 mg/L; after the third time use of the catalyst, the removal efficiency of crystal violet was 14.94% lower than that of the first time, and the zinc concentration in water was 2.75 mg/L. This shows that the catalysts still maintained high activity after three times of use. It also showed that the zinc concentration was lower than 5 mg/L in water after reaction, meeting the national discharge standard of China.

The enhanced catalytic activity for Zn⁰/Fe₃O₄ is schematically presented in Fig. 5. Magnetite is a high conductivity semiconductor, the conduction band of was 0.10 eV with almost metallic character, which is also helpful for electron transport [12,37–39]. Based on the observed data in our Fenton-like system, Zn⁰ and Fe₃O₄ can form a very efficient interface, which can promote the electron transport between Zn⁰ and Fe₃O₄. As a result, Zn⁰ in the composites was highly reactive toward H₂O₂.

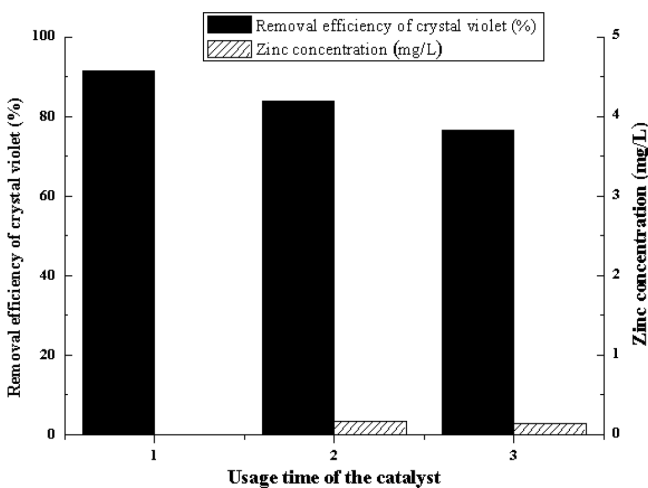


Fig. 4. Reusability of Zn⁰/Fe₃O₄ in removal of crystal violet (15 mg/L crystal violet concentration, 1.0 g/L catalyst dosage, 0.68 mmol/L H₂O₂, t = 10 min, pH = 5.0).

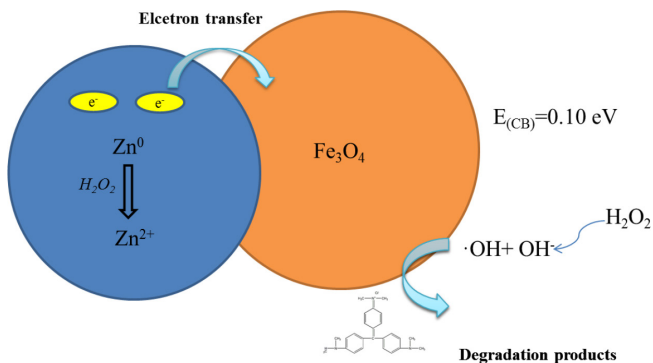


Fig. 5. Schematic diagrams for the electron-transfer process in Zn⁰-Fe₃O₄.

3.3. Effect of pH range

In addition to enhancing the catalytic activity, the development of this new Fenton-like catalyst system seeks to extend the applicable pH range. The traditional Fenton’s reagent only works well for strongly acidic conditions, which severely limits its application. It has been proven that the pH is one of the decisive factors that influence the performance of Fenton-like systems [40,41]. Many studies reported that dye decolorization in Fenton or Fenton-like systems were most efficient at pH 2.0–4.0 [4,42]. Hence, the effect of the initial pH on the decolorization of crystal violet by Zn⁰/Fe₃O₄-H₂O₂ was investigated. However, as shown in Fig. 6(a), a much lower catalyst activity was found for pH 3.0 than at higher pH; at low pH, the excess H⁺ reacts with H₂O₂ to produce H₃O₂⁺, which is stable and less active in forming the ·OH radicals [1]. Additionally, ·OH can also be consumed by excess H⁺

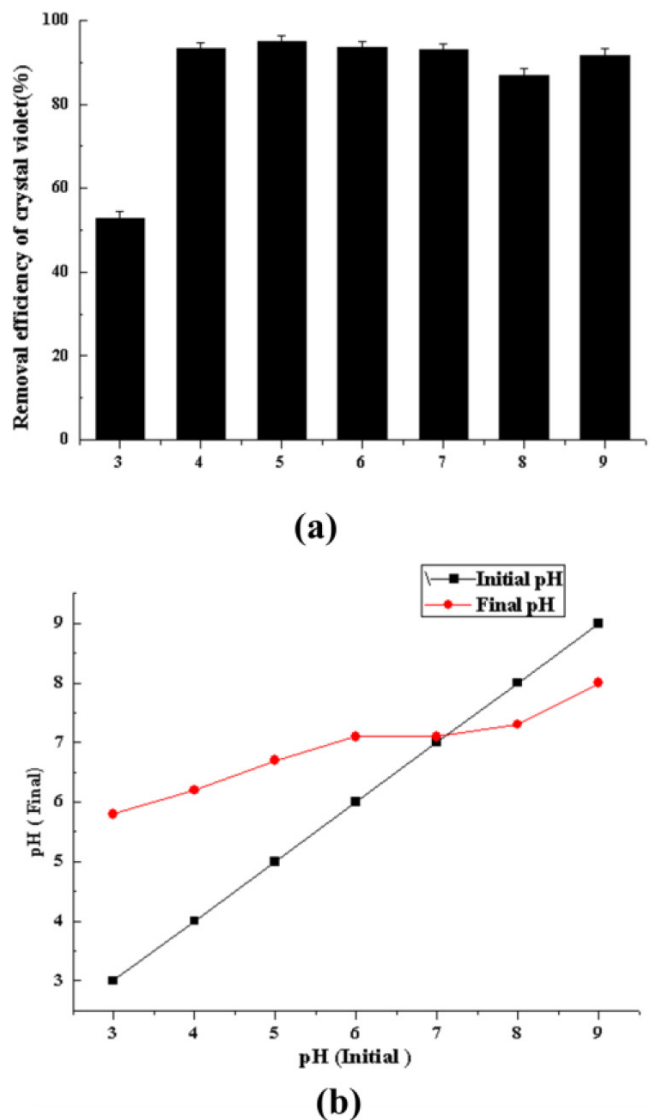


Fig. 6. (a) Effect of initial pH on the decolorization of crystal violet; (b) determination of pH_{PZC} for the catalyst (15 mg/L crystal violet concentration, 1.0 g/L catalyst dosage, 0.68 mmol/L H₂O₂, t = 10 min).

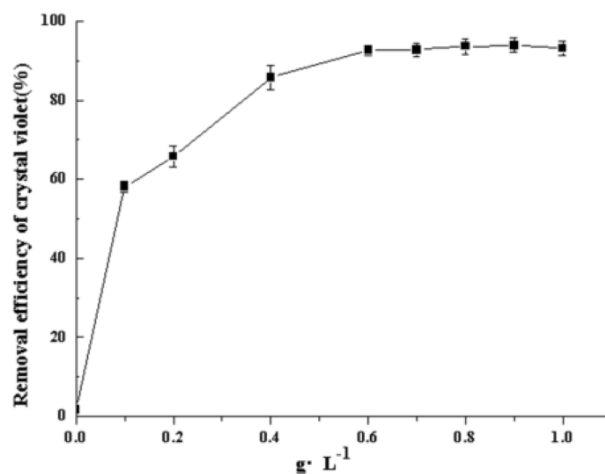
[43]. As shown in Fig. 6(b), pH_{PZC} (pH of point of zero charge) for the $\text{Zn}^0/\text{Fe}_3\text{O}_4$ catalysts was estimated about 7.0. At lower or higher pHs than pH_{PZC} , catalysts are positively charged or negatively charged, respectively [46–47]. At pH higher than pH_{PZC} , the catalyst surface is negatively charged, oxidation of cationic electron donors and acceptors are advantageous. At pH lower than pH_{PZC} , the catalyst surface is positively charged, the acidic solution provides more protons than the hydroxide solution. Fig. 6 shows that the catalytic activity of $\text{Zn}^0/\text{Fe}_3\text{O}_4$ remained high in a wide range of pH. At the initial pH value of 7.0, a complete degradation of crystal violet was observed within 10 min. The catalytic activity of $\text{Zn}^0/\text{Fe}_3\text{O}_4$ in the neutral pH range was higher than that of many reported Fenton-like catalysts [4,11,44,45]. Adaptable to a wide pH range, $\text{Zn}^0/\text{Fe}_3\text{O}_4\text{-H}_2\text{O}_2$ was superior to other Fenton-like systems. Compared with current Fenton techniques, the new $\text{Zn}^0/\text{Fe}_3\text{O}_4\text{-H}_2\text{O}_2$ system showed the advantages of a wider pH range ($4 \leq \text{pH} \leq 9$), easier separation from water and less sludge production.

3.4. Effects of operational parameters

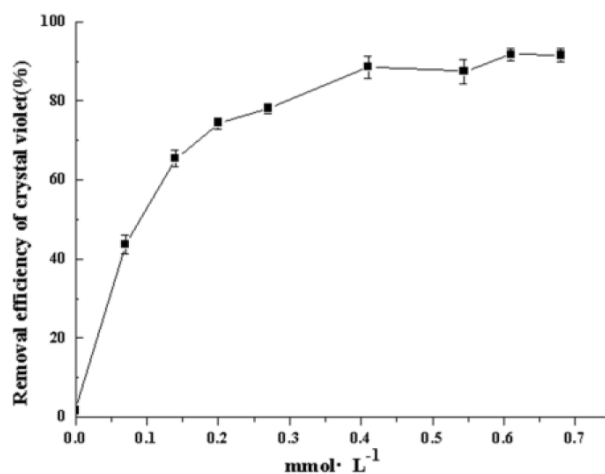
The catalyst dosage is one of the chief parameters in catalytic oxidation. In this section, the effects of $\text{Zn}^0/\text{Fe}_3\text{O}_4$ dosage are studied, and the results are illustrated in Fig. 7(a). When the $\text{Zn}^0/\text{Fe}_3\text{O}_4$ dosage rose from 0.1 to 0.7 g/L, the decolorization efficiency of crystal violet was gradually amplified. This also could be explained by the fact that increase in the catalyst dosage provided an increased number of active sites for producing electron–hole pairs [48,49] and higher concentration of $\cdot\text{OH}$ arising from H_2O_2 decomposition [50]. Once the $\text{Zn}^0/\text{Fe}_3\text{O}_4$ dosage reached 0.8 g/L, the decolorization rate remained stable. This can be explained by the consumption of $\cdot\text{OH}$ radicals by Zn^{2+} as expressed by Eq. (7), in an analogy to the $\text{Fe}^0/\text{H}_2\text{O}_2$ system [3, 11]. Therefore, 0.7 g/L was the optimal $\text{Zn}^0/\text{Fe}_3\text{O}_4$ dosage.



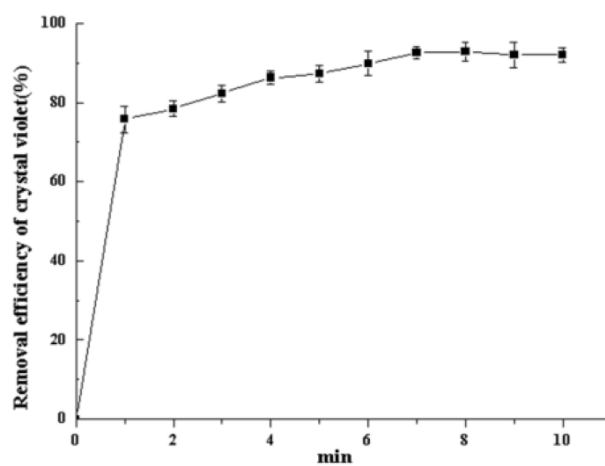
The concentration of H_2O_2 is another key parameter in Fenton-like reactions. In this section, the effect of H_2O_2 concentration was investigated. The results are shown in Fig. 7(b). When the H_2O_2 concentrations ranged from 0 to 0.07 mmol/L, the crystal violet decolorization efficiency remained less than 50% due to insufficient $\cdot\text{OH}$ [51]. When the H_2O_2 concentration rose to 0.41 mmol/L, the crystal violet decolorization efficiency was significantly enhanced. The decolorization efficiency was increased from 65.5% to 88.6% as the H_2O_2 concentration rose from 0.14 to 0.41 mmol/L. However, with a further increase of the H_2O_2 concentration from 0.54 to 0.68 mmol/L, the efficiency diminished slightly; at higher H_2O_2 concentrations, $\cdot\text{OH}$ radicals are consumed to produce perhydroxyl radicals (as shown in Eq. (8)) [52,53]. According to above analyses, H_2O_2 enhanced the degradation of pollutants due to more efficient generation of hydroxyl radical and inhibition of electron/hole pair recombination [54,55]. Hence, the optimal H_2O_2 concentration was chosen as 0.41 mmol/L.



(a)



(b)



(c)

Fig. 7. Effects of operational parameters on the decolorization of crystal violet. (a) $\text{Zn}^0/\text{Fe}_3\text{O}_4$ dosage; (b) H_2O_2 concentration; (c) reaction time (15 mg/L crystal violet concentration, $\text{pH} = 5.0$).

The effect of the reaction time on the rate of crystal violet decolorization was also investigated. As shown in Fig. 7(c), the decolorization efficiency of crystal violet rapidly reached 70% in 1 min. This rapid decolorization rate could be explained by the fast reaction between Zn^0 and H_2O_2 to produce a sufficient amount of $\cdot OH$ [56]. The efficiency reached 92.63% in 7 min. Subsequently, no significant decolorization occurred. Therefore, the optimal reaction time was 7 min, which is much shorter than the rates obtained for other Fenton-like systems [57].

3.5. Interference from co-existing pollutants

During the above experiments, the effect of the key influencing parameters on the decolorization of crystal violet was studied. The results showed that under optimal conditions, Zn^0/Fe_3O_4 had high catalytic activity. However, in real dyeing wastewater, there are various kinds of dyes present, as well as natural organic matter, and these other compounds may significantly hinder the removal of the target pollutant. Therefore, we tested the catalytic activity of Zn^0/Fe_3O_4 in water containing other typical dyes and natural organic matter.

3.5.1. Interference with other dyes

After adding other dyes into the wastewater, the catalytic oxidation of crystal violet in the $Zn^0/Fe_3O_4-H_2O_2$ system was carried out to investigate the possible effects of co-existing dyes. As shown in Figs. 8(a)–(e), crystal violet concentration was 15 mg/L, respectively, while for the results presented in Figs. 8(b)–(e), the total concentration of other dyes was 15 mg/L. Namely, the concentration of methylene blue (Fig. 8(b)) was 15 mg/L; the concentration of fuchsin acid (Fig. 8(c)) was 15 mg/L; the concentration of methyl orange (Fig. 8(d)) was 15 mg/L and the concentration of methylene blue, fuchsin acid and methyl orange (Fig. 8(e)) was 5 mg/L for each dye. Examination of Fig. 6 shows that

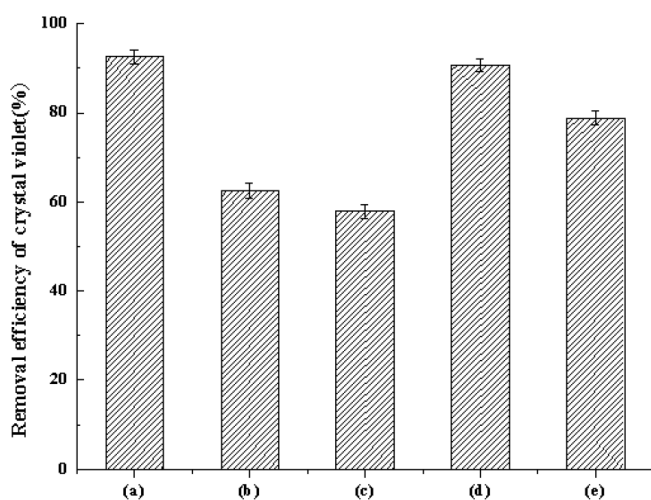


Fig. 8. Effect of co-existing dyes on the removal efficiency of crystal violet. (a) Crystal violet; (b) crystal violet + methylene blue; (c) crystal violet + fuchsin acid; (d) crystal violet + methyl orange; (e) crystal violet + methylene blue + fuchsin acid + methyl orange (0.7 g/L catalyst dosage, 0.41 mmol/L H_2O_2 , $t = 7$ min, pH = 7.0).

in the presence of interference by other dyes, the crystal violet decolorization efficiency declined but remained high. The results showed that this new Fenton-like system was still effective for the decolorization of crystal violet in wastewater containing other pollutants.

3.5.2. Interference of natural organic matter

The presence of natural organic matter greatly affects the catalytic oxidation ability of Fenton-like systems in dye wastewater [58,59]. For the results presented in Figs. 9(a)–(e), the crystal violet concentration was 15 mg/L, respectively, whereas for the results presented in Figs. 9(b)–(e), the total concentration of natural organic matter was 15 mg/L. Namely, the concentration of L-malic acid (Fig. 9(b)) was 15 mg/L; the concentration of L-histidine (Fig. 9(c)) was 15 mg/L; the concentration of humic acid (Fig. 9(d)) was 15 mg/L and the concentration of L-malic acid, L-histidine and humic acid (Fig. 9(e)) was 5 mg/L for each. During the test, L-malic acid, L-histidine and humic acid, three typical kinds of natural organic matter, were selected to examine their impact on this new Fenton-like system. Examination of the obtained results showed that the efficiency of the decolorization efficiency of crystal violet declined from 92.7% to 73.24%, 71.03% and 87.48% in the presence of L-malic acid, L-histidine and humic acid, respectively (Fig. 9). Due to the interference by all three natural organic matter types, the crystal violet decolorization efficiency decreased slightly. Overall, the catalyst still retained a high catalytic ability for H_2O_2 in the presence of natural organic matter, which is very important because these compounds exist widely in natural water systems as well as in wastewaters.

3.6. Fate of crystal violet

The absorption spectrum of the crystal violet during the Fenton-like process is shown in Fig. 10. Fig. 10(a) shows the UV–Vis spectra of crystal violet decolorization within the

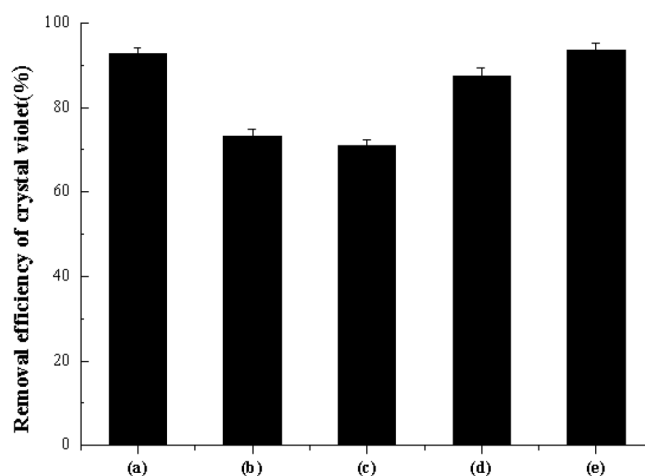


Fig. 9. Effect of co-existing natural organic matter on removal efficiency of crystal violet: (a) crystal violet; (b) crystal violet + L-malic acid; (c) crystal violet + L-histidine; (d) crystal violet + humic acid; (e) crystal violet + L-malic acid + L-histidine + humic acid (0.7 g/L catalyst dosage, 0.41 mmol/L H_2O_2 , $t = 7$ min, pH = 7.0).

time interval from 0 to 7 min in the Fenton-like system with Zn^0/Fe_3O_4 as a catalyst. The absorption spectrum of crystal violet includes one main band in the visible region with the maximum absorption at 590 nm, and another band in the UV region is located at 300 nm. The peak at 300 nm is associated with aromatic structures in the molecules, and that at 590 nm originates from an extended chromophore. Usually, the primary attack on a dye molecule by hydroxyl radicals begins with the chromophore with the formation of a colorless intermediate [60,61]. The cleavage of the chromophore structure will lead to the decay of absorbance [60]. In addition to this

rapid decolorization effect, the decay of the visible band at 300 nm is considered to be evidence of aromatic fragment degradation by oxidation in the dye molecule. The decrease of the absorption maximum peak at 590 nm may result from the formation of a series of N-demethylated intermediates [62]. Noticeably, with the increase of the discoloration time, the intensity of crystal violet absorbance continuously decreased, and intermediates of N-demethylation formed within the absorption wavelength range from 341 to 400 nm [57].

Fig. 10(b) shows the HPLC spectrum of crystal violet in Fenton-like systems. The results show that absorbance of crystal violet decreased after the reaction comparing with before the reaction. Moreover, after 7 min reaction, the concentration of TOC (total organic carbon) was 11.84 mg/L (Table 1). Organic intermediates are generated during the degradation of the target dye, contributing to the TOC. As a result, the removal efficiency of TOC changed little after 7 min. A much longer time is needed to achieve mineralization. He et al. [63] found that the decrease of TOC required much more time than the degradation of crystal violet. In this study, the removal efficiency of TOC reached 67% in 1 h.

4. Conclusions

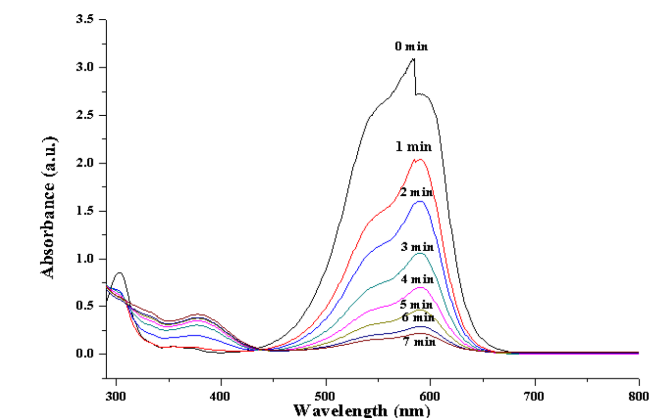
In this paper, a new Fenton-like system was prepared and used for the catalytic oxidation of crystal violet. The prepared catalyst showed that Zn^0 was successfully distributed on Fe_3O_4 and the Zn^0/Fe_3O_4 composite showed a large specific surface area and high magnetic separation ability. The prepared catalyst combines a high activity with high magnetic separation ability. The results proved $Zn^0/Fe_3O_4-H_2O_2$ to be an efficient and rapid system that decolorized crystal violet within 7 min at neutral pH and was superior to many H_2O_2 -based systems. Almost complete decolorization of crystal violet could be achieved with 0.41 mmol/L H_2O_2 and 0.7 g/L Zn^0/Fe_3O_4 and there was no residual sludge formation. Furthermore, the catalyst retained high activity in the presence of other synthetic dyes or common natural organic matter. The decolorization efficiency of crystal violet was between 57.89% and 90.81% in the presence of other synthetic dyes, the decolorization efficiency of crystal violet was between 71.03% and 93.55% in the presence of common natural organic matter. Crystal violet was completely decolorized and mostly degraded by using $Zn^0/Fe_3O_4-H_2O_2$.

Acknowledgments

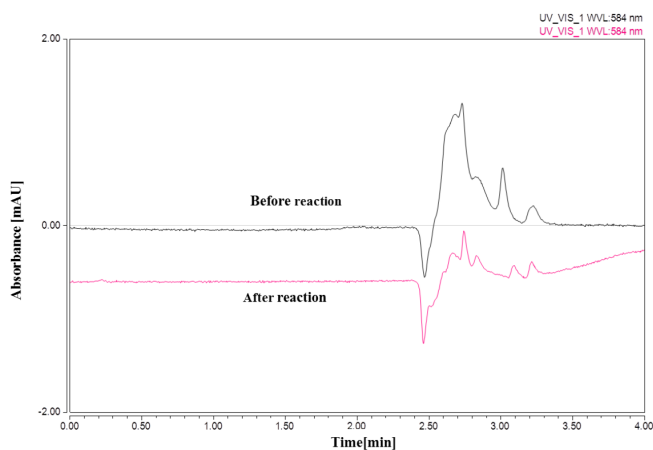
The authors thank the Beijing Natural Science Foundation (8172028) and Shenzhen Science and Technology Committee (JSKF20150901115155532) for financial support.

References

- [1] M. Tamimi, S. Qourzal, N. Barka, A. Assabbane, Y. Ait-Ichou, Methomyl degradation in aqueous solutions by Fenton's reagent and the photo-Fenton system, *Sep. Purif. Technol.*, 61 (2008) 103–108.
- [2] F. Duarte, F.J. Maldonado-Hodar, A.F. Perez-Cadenas, L.M. Madeira, Fenton-like degradation of azo-dye Orange II catalyzed by transition metals on carbon aerogels, *Appl. Catal., B*, 85 (2009) 139–147.
- [3] J.M. Fontmorin, M. Sillanpää, Bioleaching and combined bioleaching/Fenton-like processes for the treatment of urban



(a) UV-visible spectrum



(b) HPLC spectrum

Fig. 10. Absorption spectrum of crystal violet in Fenton-like systems. (a) UV-Vis spectrum and (b) HPLC spectrum.

Table 1
Removal efficiency of TOC during the catalytic degradation process

Time (min)	TOC _{final} (mg/L)	Removal efficiency (%)
0	12.94	0.0
7	11.84	8.5
60	4.27	67

- anaerobically digested sludge: removal of heavy metals and improvement of the sludge dewaterability, *Sep. Purif. Technol.*, 156 (2015) 655–664.
- [4] J.H. Deng, J.Y. Jiang, Y.Y. Zhang, X.P. Lin, C.M. Du, Y. Xiong, FeVO_4 as a highly active heterogeneous Fenton-like catalyst towards the degradation of Orange II, *Appl. Catal., B*, 84 (2008) 468–473.
- [5] A.L.T. Pham, C. Lee, F.M. Doyle, D.L. Sedlak, A silica-supported iron oxide catalyst capable of activating hydrogen peroxide at neutral pH values, *Environ. Sci. Technol.*, 43 (2009) 8930–8935.
- [6] M. Kallel, C. Belaid, T. Mechichi, M. Ksibi, B. Elleuch, Removal of organic load and phenolic compounds from olive mill wastewater by Fenton oxidation with zero-valent iron, *Chem. Eng. J.*, 150 (2009) 391–395.
- [7] T. Zhou, Y.Z. Li, J. Ji, Oxidation of 4-chlorophenol in a heterogeneous zero valent iron/ H_2O_2 Fenton-like system: kinetic, pathway and effect factors, *Sep. Purif. Technol.*, 62 (2008) 551–558.
- [8] G.B. Ortiz de la Plata, O.M. Alfano, A.E. Cassano, Decomposition of 2-chlorophenol employing goethite as Fenton catalyst II: reaction kinetics of the heterogeneous Fenton and photo-Fenton mechanisms, *Appl. Catal., B*, 95 (2010) 14–25.
- [9] M.C. Pereira, L.C.A. Oliveira, E. Murad, Iron oxide catalysts: Fenton and Fenton-like reactions—a review, *Clay Miner.*, 47 (2012) 285–302.
- [10] L. Xu, J. Wang, Degradation of 2,4,6-trichlorophenol using magnetic nanoscaled $\text{Fe}_3\text{O}_4/\text{CeO}_2$ composite as a heterogeneous Fenton-like catalyst, *Sep. Purif. Technol.*, 149 (2015) 255–264.
- [11] S.X. Zhang, X.L. Zhao, H.Y. Niu, Y.L. Shi, Y.Q. Cai, G.B. Jiang, Superparamagnetic Fe_3O_4 nanoparticles as catalysts for the catalytic oxidation of phenolic and aniline compounds, *J. Hazard. Mater.*, 167 (2009) 560–566.
- [12] R.C.C. Costa, F.C.C. Moura, J.D. Ardisson, J.D. Fabris, R.M. Lago, Highly active heterogeneous Fenton-like systems based on $\text{Fe}^0/\text{Fe}_3\text{O}_4$ composites prepared by controlled reduction of iron oxides, *Appl. Catal., B*, 83 (2008) 131–139.
- [13] A. Khataee, R. Darvishi Cheshmeh Soltani, Y. Hanifehpour, M. Safarpour, H. Gholipour Ranjbar, S.W. Joo, Synthesis and characterization of dysprosium-doped ZnO nanoparticles for photocatalysis of a textile dye under visible light irradiation, *Ind. Eng. Chem. Res.*, 53 (2014) 1924–1932.
- [14] A. Khataee, R.D.C. Soltani, A. Karimi, S.W. Joo, Sonocatalytic degradation of a textile dye over Gd-doped ZnO nanoparticles synthesized through sonochemical process, *Ultrason. Sonochem.*, 23 (2015) 219–230.
- [15] S. Anju, K. Jyothi, S.Y. Sindhu Joseph, E. Yesodharan, Ultrasound assisted semiconductor mediated catalytic degradation of organic pollutants in water: comparative efficacy of ZnO, TiO_2 and ZnO- TiO_2 , *Res. J. Recent Sci.*, 1 (2012) 191–201.
- [16] N. Ertugay, F.N. Acar, The degradation of Direct Blue 71 by sono, photo and sonophotocatalytic oxidation in the presence of ZnO nanocatalyst, *Appl. Surf. Sci.*, 318 (2014) 121–126.
- [17] A. Khataee, S. Saadi, B. Vahid, S.W. Joo, B.K. Min, Sonocatalytic degradation of Acid Blue 92 using sonochemically prepared samarium doped zinc oxide nanostructures, *Ultrason. Sonochem.*, 29 (2016) 27–38.
- [18] H.Y. He, J. Fe, J. Lu, High photocatalytic and photo-Fenton-like activities of ZnO-reduced graphene oxide nanocomposites in the degradation of malachite green in water, *IET Micro Nano Lett.*, 10 (2015) 389–394.
- [19] T.T. Vu, G. Marban, Sacrificial template synthesis of high surface area metal oxides. Example: an excellent structured Fenton-like catalyst, *Appl. Catal., B*, 152 (2014) 51–58.
- [20] A. Akcil, F. Vegliob, F. Ferella, M.D. Okudan, A. Tuncuk, A review of metal recovery from spent petroleum catalysts and ash, *Waste Manage.*, 45 (2015) 420–433.
- [21] M. Marafi, A. Stanislaus, Spent catalyst waste management: a review Part I—developments in hydroprocessing catalyst waste reduction and use, *Resour. Conserv. Recycl.*, 52 (2008) 859–873.
- [22] H.Y. Zhu, Y.Q. Fu, R. Jiang, J.H. Jiang, L. Xiao, G.M. Zeng, Y. Wang, Adsorption removal of Congo red onto magnetic cellulose/ Fe_3O_4 /activated carbon composite: equilibrium, kinetic and thermodynamic studies, *Chem. Eng. J.*, 173 (2011) 494–502.
- [23] X. Zhang, P.Y. Zhang, Z. Wu, L. Zhang, G.M. Zeng, C.J. Zhou, Adsorption of methylene blue onto humic acid-coated Fe_3O_4 nanoparticles, *Colloids Surf. A*, 435 (2013) 85–90.
- [24] L. Wang, J. Li, Z. Wang, L. Zhao, Q. Jiang, Low-temperature hydrothermal synthesis of $\alpha\text{-Fe}/\text{Fe}_3\text{O}_4$ nanocomposite for fast Congo red removal, *Dalton Trans.*, 42 (2013) 2572–2579.
- [25] A. Mittal, J. Mittal, A. Malviya, D. Kaur, Adsorption of hazardous dye crystal violet from wastewater by waste materials, *J. Colloid Interface Sci.*, 343 (2010) 463–473.
- [26] A. Nezamzadeh-Ejhieh, Z. Banan, A comparison between the efficiency of CdS nanoparticles/zeolite A and CdO/zeolite A as catalysts in photodecolorization of crystal violet, *Desalination*, 279 (2011) 146–151.
- [27] A. Safavi, S. Momeni, Highly efficient degradation of azo dyes by palladium/hydroxyapatite/ Fe_3O_4 nanocatalyst, *J. Hazard. Mater.*, 201 (2012) 125–131.
- [28] M.T. Chaudhry, M. Zohaib, N. Rauf, S.S. Tahir, S. Parvez, Biosorption characteristics of *Aspergillus fumigatus* for the decolorization of triphenylmethane dye acid violet 49, *Appl. Microbiol. Biotechnol.*, 98 (2014) 3133–3141.
- [29] A. Adak, M. Bandyopadhyay, A. Pal, Removal of crystal violet dye from wastewater by surfactant-modified alumina, *Sep. Purif. Technol.*, 44 (2005) 139–144.
- [30] K.P. Singh, S. Gupta, A.K. Singh, S. Sinha, Optimizing adsorption of crystal violet dye from water by magnetic nanocomposite using response surface modeling approach, *J. Hazard. Mater.*, 186 (2011) 1462–1473.
- [31] A. Nezamzadeh-Ejhieh, Z. Banan, Sunlight assisted photodecolorization of crystal violet catalyzed by CdS nanoparticles embedded on zeolite A, *Desalination*, 284 (2012) 157–166.
- [32] J. Xu, L. Tan, S.A. Baig, D. Wu, X. Lv, X. Xu, Dechlorination of 2,4-dichlorophenol by nanoscale magnetic Pd/Fe particles: effects of pH, temperature, common dissolved ions and humic acid, *Chem. Eng. J.*, 231 (2013) 26–35.
- [33] A. Nezamzadeh-Ejhieh, Z. Banan, Photodegradation of dimethyldisulfide by heterogeneous catalysis using nanoCdS and nanoCdO embedded on the zeolite A synthesized from waste porcelain, *Desal. Wat. Treat.*, 52 (2014) 3328–3337.
- [34] B. Khodadadi, M. Bordbar, Sonochemical synthesis of undoped and Co-doped ZnO nanostructures and investigation of optical and photocatalytic properties, *Iran. J. Catal.*, 6 (2016) 37–42.
- [35] J. Sadiq, M. Mohamed, N.A. Samson, Reflux condensation synthesis and characterization of Co_3O_4 nanoparticles for photocatalytic applications, *Iran. J. Catal.*, 4 (2014) 219–226.
- [36] M. Bahrami, A. Nezamzadeh-Ejhieh, Effect of the supported ZnO on clinoptilolite nano-particles in the photodecolorization of semi-real sample bromothymol blue aqueous solution, *Mater. Sci. Semicond. Process.*, 30 (2015) 275–284.
- [37] J. Esmaili-Hafshejani, A. Nezamzadeh-Ejhieh, Increased photocatalytic activity of Zn(II)/Cu(II) oxides and sulfides by coupling and supporting them onto clinoptilolite nanoparticles in the degradation of benzophenone aqueous solution, *J. Hazard. Mater.*, 316 (2016) 194–203.
- [38] H. Derikvandi, A. Nezamzadehejhieh, Increased photocatalytic activity of NiO and ZnO in photodegradation of a model drug aqueous solution: effect of coupling, supporting, particles size and calcination temperature, *J. Hazard. Mater.*, 321 (2017) 629–638.
- [39] H. Derikvandi, A. Nezamzadeh-Ejhieh, A comprehensive study on electrochemical and photocatalytic activity of $\text{SnO}_2\text{-ZnO}$ /clinoptilolite nanoparticles, *J. Mol. Catal. A Chem.*, 426 (2017) 158–169.
- [40] I.A. Katsoyiannis, T. Ruettimann, S.I. Hug, pH dependence of Fenton reagent generation and As (III) oxidation and removal by corrosion of zero valent iron in aerated water, *Environ. Sci. Technol.*, 42 (2008) 7424–7430.
- [41] R. Su, J. Sun, Y.P. Sun, K.J. Deng, D.M. Cha, D.Y. Wang, Oxidative degradation of dye pollutants over a broad pH range using hydrogen peroxide catalyzed by $\text{FePz}(\text{dtnCl})_4$, *Chemosphere*, 77 (2009) 1146–1151.
- [42] X. Zhong, S. Royer, H. Zhang, Q. Huang, L. Xiang, S. Valange, J. Barrault, Mesoporous silica iron-doped as stable and efficient

- heterogeneous catalyst for the degradation of C.I. acid orange 7 using sono-photo-Fenton process, *Sep. Purif. Technol.*, 80 (2011) 163–171.
- [43] B. Lodha, S. Chaudhari, Optimization of Fenton-biological treatment scheme for the treatment of aqueous dye solutions, *J. Hazard. Mater.*, 148 (2007) 459–466.
- [44] S.J. Yang, H.P. He, D.Q. Wu, D. Chen, Y.H. Ma, X.L. Li, P. Yuan, Degradation of methylene blue by heterogeneous Fenton reaction using titanomagnetite at neutral pH values: process and affecting factors, *Ind. Eng. Chem. Res.*, 48 (2009) 9915–9921.
- [45] S.D. Chatterjee, A. Katafias, Degradation of methylene blue by the [RuIII(hedtra)(H₂O)]/H₂O₂ catalytic system, *Curr. Catal.*, 3 (2014) 82–87.
- [46] H. Zabihi-Mobarakeh, A. Nezamzadeh-Ejhieh, Application of supported TiO₂ onto Iranian clinoptilolite nanoparticles in the photodegradation of mixture of aniline and 2, 4-dinitroaniline aqueous solution, *J. Ind. Eng. Chem.*, 26 (2015) 315–321.
- [47] N. Ajoudanian, A. Nezamzadeh-Ejhieh, Enhanced photocatalytic activity of nickel oxide supported on clinoptilolite nanoparticles for the photodegradation of aqueous cephalixin, *Mater. Sci. Semicond. Process.*, 36 (2015) 162–169.
- [48] S. Mousavi-Mortazavi, A. Nezamzadeh-Ejhieh, Supported iron oxide onto an Iranian clinoptilolite as a heterogeneous catalyst for photodegradation of furfural in a wastewater sample, *Desal. Wat. Treat.*, 57 (2016) 10802–10814.
- [49] P. Mohammadyari, A. Nezamzadeh-Ejhieh, Supporting of mixed ZnS–NiS semiconductors onto clinoptilolite nanoparticles to improve its activity in photodegradation of 2-nitrotoluene, *RSC Adv.*, 5 (2015) 75300–75310.
- [50] Q. Liao, J. Sun, L. Gao, Degradation of phenol by heterogeneous Fenton reaction using multi-walled carbon nanotube supported Fe₂O₃ catalysts, *Colloids Surf., A*, 345 (2009) 95–100.
- [51] N.K. Daud, B.H. Hameed, Decolorization of acid red 1 by Fenton-like process using rice husk ash-based catalyst, *J. Hazard. Mater.*, 176 (2010) 938–944.
- [52] J.A. Melero, G. Calleja, F. Martinez, R. Molina, M. Pariente, Nanocomposite Fe₂O₃/SBA-15: an efficient and stable catalyst for the catalytic wet peroxidation of phenolic aqueous solutions, *Chem. Eng. J.*, 131 (2007) 245–256.
- [53] W. Luo, L. Zhu, N. Wang, H. Tang, M. Cao, Y. She, Efficient removal of organic pollutants with magnetic nanoscaled BiFeO₃ as a reusable heterogeneous Fenton-like catalyst, *Environ. Sci. Technol.*, 44 (2010) 1786–1791.
- [54] Z.A. Mirian, A. Nezamzadeh-Ejhieh, Removal of phenol content of an industrial wastewater via a heterogeneous photodegradation process using supported FeO onto nanoparticles of Iranian clinoptilolite, *Desal. Wat. Treat.*, 57 (2016) 16483–16494.
- [55] A. Nezamzadeh-Ejhieh, Z. Ghanbari-Mobarakeh, Heterogeneous photodegradation of 2,4-dichlorophenol using FeO doped onto nano-particles of zeolite P, *J. Ind. Eng. Chem.*, 21 (2015) 668–676.
- [56] N. Ertugay, E. Malkoc, Removal of acid red 92 by homogeneous and heterogenous Fenton and Fenton-like processes, *J. Selcuk Univ. Nat. Appl. Sci.*, 3 (2013) 473–489.
- [57] H.J. Fan, S.T. Huang, W.H. Chung, J.L. Jan, W.Y. Lin, C.C. Chen, Degradation pathways of crystal violet by Fenton and Fenton-like systems: condition optimization and intermediate separation and identification, *J. Hazard. Mater.*, 171 (2009) 1032–1044.
- [58] N. Lubick, Cap degrade: a reactive nanomaterial barrier also serves as a cleanup tool, *Environ. Sci. Technol.*, 43 (2009) 235–235.
- [59] M.S.H. Mak, P. Rao, I. Lo, Zero-valent iron and iron oxide-coated sand as a combination for removal of co-present chromate and arsenate from groundwater with humic acid, *Environ. Pollut.*, 159 (2011) 377–382.
- [60] J. Wu, H. Gao, S. Yao, L. Chen, Y. Gao, H. Zhang, Degradation of crystal violet by catalytic ozonation using Fe/activated carbon catalyst, *Sep. Purif. Technol.*, 147 (2015) 179–185.
- [61] I. Siminiceanu, C.I. Alexandru, E. Brillas, A kinetic model for the crystal violet mineralisation in water by the electro-Fenton process, *Environ. Eng. Manage. J.*, 7 (2008) 9–12.
- [62] H. Zhang, J. Wu, Z. Wang, D. Zhang, Electrochemical oxidation of Crystal Violet in the presence of hydrogen peroxide, *J. Chem. Technol. Biotechnol.*, 85 (2010) 1436–1444.
- [63] H. He, S. Yang, K. Yu, Y. Ju, C. Sun, L. Wang, Microwave induced catalytic degradation of crystal violet in nano-nickel dioxide suspensions, *J. Hazard. Mater.*, 173 (2010) 393–400.